2D numerical forced-motion simulations of vortex-induced vibration wakes: Toward understanding the onset of three-dimensional effects

Meysam Rajabi*, Erdem Aktosun, Brian Mingels***, Jason Dahl****, Ersegun Deniz Gedikli*****

***University of Hawaii at Manoa, HI, US**, meysam@hawaii.edu

****İzmir Kâtip Çelebi University, İzmir, Turkiye,** erdem.aktosun@ikcu.edu.tr

*****University of Rhode Island, RI, US,** brian_mingels@uri.edu

******University of Rhode Island, RI, US,** jmdahl@uri.edu

*******University of Hawaii at Manoa, HI, US**, egedikli@hawaii.edu

Abstract

In this study, we conducted numerical forced-motion simulations of cylinder motions typically experienced during cross-flow vortex-induced vibrations (VIV) using the boundary data immersion method (BDIM). Our initial focus was on validating the simulations for the case of one-degree-of-freedom (1-DOF) forced motion of a circular cylinder in a free stream. The results demonstrated that the observations of wake patterns and forces obtained from the simulations were realistic and aligned well with experimental data at low reduced velocity and low amplitudes, primarily where the cylinder experiences a '2S' type wake. However, as the reduced velocity and amplitude increased, the influence of three-dimensional (3D) effects became more prominent, and the simulations were unable to accurately capture these effects, resulting in significant deviation of the wake and forces from those observed in equivalent experiments. Therefore, it becomes crucial to comprehend the conditions under which the onset of 3D effects occurs in order to develop precise prediction models. Our research highlights the successful validation of 2D simulations for 1-DOF VIV, particularly at low velocities and amplitudes, but highlights where this type of model breaks down. The limitations of 2D simulations in capturing 3D effects emphasize the need for a deeper understanding of the conditions leading to these effects in order to enhance the accuracy of prediction models.

Keywords: VIV, fluid-structure interactions, numerical simulations, boundary data immersion method

1. Introduction

Vortex-induced vibrations (VIVs) of a circular cylinder have been subject to extensive study over recent decades in the context of ocean engineering applications. This phenomenon arises when an object is immersed in a flow, and the varying lift force caused by the formation of vortices in the wake leads to the object vibrating. Early VIV research focused on oscillations exclusively in cross-flow directions, often referred to as one-degree-of-freedom (1DOF) systems. Later, focus shifted to two-degree-of-freedom (2DOF) systems in which the structure oscillates in both in-line and cross-flow directions. Several fundamental studies discusses the significance of VIV are Bearman, 1984, 2011; Carberry et al., 2005; Gabbai & Benaroya, 2005; Griffin & Ramberg, 1982; Parkinson, 1989; Sarpkaya, 1979, 2004; Williamson & Govardhan, 2004, 2008. The findings from past VIV research have been used to guide the design and optimization of offshore structures, improve their performance and reliability, and reduce the potential risks associated with VIV. Investigating the physics of vortex shedding from the cylinder and understanding the formation and shedding of vortices in the wake helps in predicting the vibration characteristics and identifying strategies to modify the vortex-shedding process.

This research focuses primarily on validating 1-DOF VIV simulations using the boundary data immersion method (Weymouth & Yue, 2011) and comparing the results to 1-DOF experiments (Morse & Williamson, 2009). Most numerical studies overlook the fact that bluff body investigations involve three-dimensional effects that may alter the hydrodynamic and dynamic response of the body under specific conditions. For instance, as the Reynolds number increases in VIV, vortices shedding downstream may exhibit hysteretic behavior resulting wake instabilities or wake patterns that can also vary along the length of the body resulting complex body motions (Jiang et al., 2018; Williamson, 1996). Even in simple simulations of flow past a circular cylinder, there are significant challenges reproducing the realistic wake and forcing parameters (Font Garcia et al., 2019; Yang & Stremler, 2016).

An illustration of 1-DOF forced motion experiments was presented in the work of Gopalkrishnan (1993). The experiment involved towing a cylinder at a constant forward speed while simultaneously subjecting it to a forced oscillation perpendicular to the direction of towing. The motion was characterized by a sinusoidal pattern, and variations were made in both the amplitude and frequency of the motion. In the meantime, measurements were taken to record the forces exerted on the body during the experiments. Due to the experimental nature of the work, its response is inherently three-dimensional.

Many studies have been carried out to address similar problems involving a cylinder undergoing to a free stream and forced to do a prescribed sinusoidal motion perpendicular to the flow direction. Vikestad et al. (2000) conducted a series of experiments in a tow tank at higher Reynolds numbers when compared to Gopalkrishnan (1993). These experiments showed fluctuations in the measured forces due to the changes in Reynolds number values.

Morse and Williamson (2009) conducted a series of forced vibration tests to predict the motion of an elastically mounted circular cylinder immersed in a fluid flow and analyze the patterns in their wake.

They created high-resolution contour plots of fluid forcing magnitude and phase, as well as other related quantities, in the plane of normalized amplitude and wavelength. The findings revealed clear discontinuities in the force contours, identifying different fluid forcing regimes that show similarities to boundaries separating vortex shedding modes. Additionally, a novel observation of an overlap region with distinct vortex formation modes was identified, with intermittent switching between the modes even as the cylinder oscillates with constant amplitude and frequency. Understanding this overlap region is crucial for comprehending the behavior of free vibration systems at peak amplitude response. This work and the wake patterns presented in this work is also the basis of our study for 1-DOF validation.

In rigid cylinder VIV there are mainly three distinct response branches emerge with different response amplitudes (Williamson and Govardhan, 2008). These branches are referred to as the initial branch, upper branch, and lower branch. Later, Morse and Williamson (2009) introduced a new branch called $2P_{OVERLAP}$ which occurs around the reduced velocity of 5, and updated the vortex shedding regime map. The initial branch displays amplitude modulation, indicating the presence of two frequencies. In the upper and lower branches, the vortex-shedding frequency becomes synchronized with the response frequency of the cylinder. Additionally, experimental investigations have identified a relationship between the 2S mode (two single vortices shed per cycle) and the initial branch, as well as the 2P mode (two paired vortices shed per cycle) and the lower branch. The 2P mode is also observed in the upper branch, although the second vortex of each pair is significantly weaker than the first one (Morse & Williamson, 2009). However, the underlying reasons of the upper branch's separation from the lower branch, as well as the random characteristics of the response remain poorly understood. Furthermore, few numerical studies have reported the presence of the 2P mode (Pan et al., 2007). The existence of the 2P mode as a steady-state pattern is still a subject of debate. Significant disparities are apparent in the outcomes achieved through various prediction methodologies as a result of differing assumptions and empirical databases employed in empirical approaches. Conversely, due to uncertainties inherent in computational fluid dynamics techniques concerning the modeling of vortex shedding in conjunction with the dynamic response of the structure, further comprehensive research efforts are imperative to enhance our comprehension of VIV in long and slender marine structures. This study aims to investigate how controlled vibration affects fluid force and wake modes. We also investigate the effects of prescribing a sinusoidal motion for a cylinder that moves transversely to a free stream, and whether BDIM-based numerical simulations can successfully replicate and enhance our understanding of this simple problem. Furthermore, we discuss the limitations found in prior numerical studies and explore underlying reasoning behind their inability to comprehensively capture all the requirements of 2P mode.

2. Numerical Method Description

In order to address this fluid-structure interaction problem, the numerical Boundary Data Immersion Method (BDIM) is employed for solving the two-dimensional Navier-Stokes equations by incorporating

precise body boundary conditions of solid entities into the fluid domain. A comprehensive explanation of how this method solves the governing equations of the flow and validation of this method including for the case of flow past a circular cylinder can be found in these studies (Maertens & Weymouth, 2015; Weymouth & Yue, 2011).

BDIM is a numerical method based on a general integration kernel formulation that analytically combines the field equations of each domain and interfacial conditions. By leveraging BDIM, it is possible to achieve high levels of accuracy and reliability in simulations of intricate problems, while minimizing the computational complexity, without requiring a substantial increase in computational resources. BDIM modifies the equations of motion to consider the interaction between the fluid and solid components, enabling their solution on a straightforward numerical grid. In other words, we use BDIM to adjust the equations and solve them efficiently on a simple grid, facilitating the simulation of fluid-solid interactions. We employed the implicit Large Eddy Simulation (ILES) technique (Margolin, 2014) to represent the smaller scales below the finite grid spacing. The purpose was to circumvent the challenges associated with selecting and parameterizing standard turbulence models. Despite its straightforwardness, ILES has been demonstrated to offer improved effective subgrid resolution compared to explicit LES models (Aspden et al., 2008). However, similar to other LES models, it necessitates explicit time-stepping and poses challenges in scaling up for high Reynolds number flows.

The simulation environment is based on the Navier-Stokes equations and the general form of Navier-Stokes equations can be written as:

$$\rho \frac{Du}{Dt} = -\frac{dp}{dx} + \mu \frac{d^2u}{dx^2} \tag{1}$$

where u is the local fluid velocity vector, p is the local pressure of the fluid, ρ and μ are the fluid density and viscosity, D/Dt is the material derivative, d/dx is gradient, and d^2/dx^2 is Laplacian.

Within the solver framework, both the fluid and solid governing mechanical equations are employed in a non-dimensional form (Weymouth, 2015). This approach involves scaling the equations based on the uniform flow velocity and the grid size. The reason for this non-dimensionalization is that parameters related to size or time can be customized by the user and cannot be directly incorporated into the governing equations. By employing non-dimensionalization, the solver ensures the robustness of grid-based parameters. It is important to note that scaling is necessary for engineering coefficients such as length, time-step, and fluid viscosity. Therefore, the code is scaled using fixed numerical parameters, which include the grid cell dimension (n), the uniform flow velocity (U), and the fluid density (ρ). As a result of this scaling, the variables become non-dimensional, leading to a more streamlined and standardized representation of the problem. After applying scaling to the code using fixed numerical parameters the resulting non-dimensional variables are defined as $x = x_0/n$ and $t = t_0 U/n$, where the non-dimensional variables denoted as x and t, which represent distances and times, respectively. These

non-dimensional quantities are computed based on the variables x_0 and t_0, which are the original dimensional distances and time.

The careful selection of grid resolution (n) and time step (Δt) is of utmost importance to accurately capture the complexities of the problem and obtain reliable results. In this study, different grid resolutions (130×130, 258×258, 514×514, and 1024×1024) and time steps (0.05, 0.08, 0.1, 0.12, and 0.15) were explored to optimize the computational domain. Ultimately, the grid cell dimension of $n = 258 \times 258$ and time step $\Delta t = 0.1$ were chosen based on their ability to ensure stability and accuracy in simulating wake mode and flow forces. Furthermore, the entire simulation was conducted for a total duration of 10 seconds, a time frame determined based on achieving a stable observation of wake patterns and forces.

In the context of a 2D viscous fluid, we examine a body subject to a predetermined velocity. By employing a symmetric kernel with a specified width for the convolution process and retaining terms up to second-order, we can state:

$$\vec{u}_\epsilon = \mu_0 \vec{f} + (1 - \mu_0)\vec{b} + \mu_1 \frac{\partial}{\partial n}(\vec{f} - \vec{b}) \tag{2}$$

$$\vec{\nabla} \cdot \vec{u}_\epsilon = (1 - \mu_0)\vec{\nabla} \cdot \vec{b} - \mu_1 \frac{\partial}{\partial n}(\vec{\nabla} - \vec{b}) \tag{3}$$

The updated equations for the velocity in the fluid and body domains are denoted as f and b, respectively. The zeroth moment (μ_0) and the first moment (μ_1) of the kernel function, computed with respect to the fluid domain, play a significant role in these equations (Weymouth, 2015; Weymouth & Yue, 2011). The convoluted velocity update Equation (2) assumes the form of a mixing equation, with the fluid equation applied in the fluid domain (where $\mu_0 = 1$ and $\mu_1 = 0$), the body equation employed in the body domain (where $\mu_0 = \mu_1 = 0$), and a combination of the two within the boundary region.

Furthermore, the velocity divergence Equation (3) is utilized to determine the pressure needed to satisfy the divergence condition in both domains. This approach allows for the modeling of volume-changing bodies encountered in complex fluid-structure interaction problems as such as in wind energy (morphing wind turbine blades), underwater marine robotics and biological flow problems. By employing these equations, the fluid and body interactions can be effectively characterized and simulated. In this formulation, there are three key observations to highlight: firstly, the inclusion of the normal derivative term in the velocity equation, particularly in the boundary region, facilitates precise simulation of boundary layers, including accurate prediction of separation. Secondly, the involvement of kernel moments leads to a variable coefficient Poisson equation for the pressure, which implicitly enforces the appropriate pressure boundary conditions and greatly enhances the accuracy of force prediction. Lastly, the velocity equation for the body ($\vec{b}$) can be seamlessly integrated with the fluid state, enabling simulations that involve prescribed or predicted fluid-structure interactions. These aspects collectively

contribute to the robustness and versatility of the proposed methodology (Maertens & Weymouth, 2015; Weymouth, 2014; Weymouth & Yue, 2011).

3. Numerical Analysis and Results

This section presents a set of 960 two-dimensional simulation runs conducted to investigate the forced motion of a cylinder under a uniform flow, specifically focusing on one degree of freedom. Throughout the entire simulation, a fixed Reynolds number of 4000 has been selected as the operating condition as in Morse and Williamson (2009). Table 1 shows the simulation parameters which are used to conduct simulations. The experimental datasets from the study conducted by Morse & Williamson (2009) are considered the basis for exploring two-dimensional simulations aim at capturing various wake modes that may occur during the forced motion of a cylinder in one degree of freedom. Fig. 1 shows comparison of 2D simulations results with experimental data in the map of vortex-shedding regimes. The presented map illustrates the various wake modes generated by considering the oscillation amplitude of the cylinder in non-dimensional form ($A^* = A_y/D$) and the reduced velocity (V_r) as key parameters. It provides a visual representation of how different combinations of these parameters lead to distinct wake patterns. In this map, the regions labeled as P+S, 2S, 2S(C), and 2P correspond to experimental data, while the differently colored points represent simulation results from the present study. Each point on the map represents a separate simulation run, showcasing the outcomes obtained in relation to the respective parameters. The points on the map are categorized by color to indicate the level of agreement between the numerical simulations and the experimental wake modes. The green points indicate that the numerical simulations successfully captured the corresponding wake modes observed in the experiments. On the other hand, the red points signify instances where the numerical simulations failed to reproduce the observed wake modes. The presence of orange-colored points near the boundaries of P+S and 2S(C) regions indicates a noteworthy observation. This scenario can be characterized as a regime where wake modes overlap. In the 2S(C) area, the numerical simulations are still capable of capturing the P+S mode as the amplitude increased for a given reduced velocity. This observation notes that these boundaries are not necessarily fixed and in the present study, can be significantly affected by the details of the numerical method. Mores and Williamson (2009) noted that these boundaries shift as a function of Reynolds number and in 2D simulations, where turbulent effects can be strongly affected by increasing Reynolds number or the chosen turbulence modeling technique, it is unsurprising that irregular comparisons near these boundaries are observed. Additionally, the yellow points indicate a lack of synchronized patterns in both the numerical simulations and the experimental results. The analysis reveals that as the reduced velocity and oscillation amplitude increase, the capability to accurately capture wake modes decreases. This phenomenon is particularly evident in the 2P region of the parameter space. The findings suggest that higher levels of reduced velocity and oscillation

amplitude pose challenges for numerical simulations in effectively reproducing the observed wake modes associated with VIV. These findings contribute to advancing our understanding of VIV and highlight the need for further investigation in this area. The inability to capture the 2P wake mode can be attributed to the comparison between 2D numerical models and 3D experimental observations. As the oscillation amplitude (A^*) and reduced velocity (V_r) increase, the limitations of 2D models become apparent in accurately reproducing the 3D nature of the phenomenon. The results indicate that there are significant differences between the two-dimensional simulations and the three-dimensional experimental conditions, emphasizing the necessity of considering the full three-dimensional aspects in capturing the intricacies of wake modes. This finding underscores the importance of incorporating three-dimensional modeling approaches in future studies to better understand the complex dynamics of VIV.
To calculate the hydrodynamic coefficients, the measured hydrodynamic lift force can be modeled as a sinusoid with a phase shift and then the force can be divided into two components 1) a nondimensional force in phase with velocity (CL_v) governing the excitation of the structure, 2) a force in phase with acceleration (CL_a) governing the effect mass of the system.
Fig. 2 presents a comparison between 2D simulation results and experimental data for the force in phase with velocity (CL_v), obtained by decomposing the transverse force coefficient. Equation (4) calculates Cl_v values using the normalized inner product of their time histories. To avoid bias, the mean in the lift signal is removed before computation. Inner product is separately computed for each cycle, and the force coefficients are averaged over N cycles as in Aktosun et al. (2023) and Gedikli & Dahl (2014).

$$Cl_v = \frac{1}{N}\sum_{i=1}^{N}\sqrt{\frac{2}{T_i}}\frac{Cl_i(t)\cdot\dot{y}_i(t)}{\sqrt{\dot{y}_i(t)\cdot\dot{y}_i(t)}} \tag{4}$$

where T is the window length for the inner product.

Table 1. Simulation parameters ((Morse & Williamson, 2009)).

Reduced velocity	$Vr = U/fD$
Normalized amplitude	$A^* = A_y/D$
Transverse force coefficient	$C_y = F_y/0.5\rho U^2 D$
Reynolds number	$\rho UD/\mu$
Force in phase with velocity	$CL_v = C_y \sin \emptyset$

A selection of representative points from all simulation runs is chosen for comparison with the experimental values, serving as a validation of the credibility of the wake mode depicted in Fig. 1. The crucial aspect of this comparison lies in instances where the wake mode undergoes a phase change, resulting in a change in the sign of CL_v values. The results demonstrate that CL_v values in regions where the wake modes were valid closely approximate the experimental values. In contrast, regions with CL_v values close to zero exhibit a change in sign that is also observed in the numerical simulation results.

However, similar to the wake mode analysis in Fig. 1, the numerical simulation values deviate significantly from the laboratory values in the 2P region.

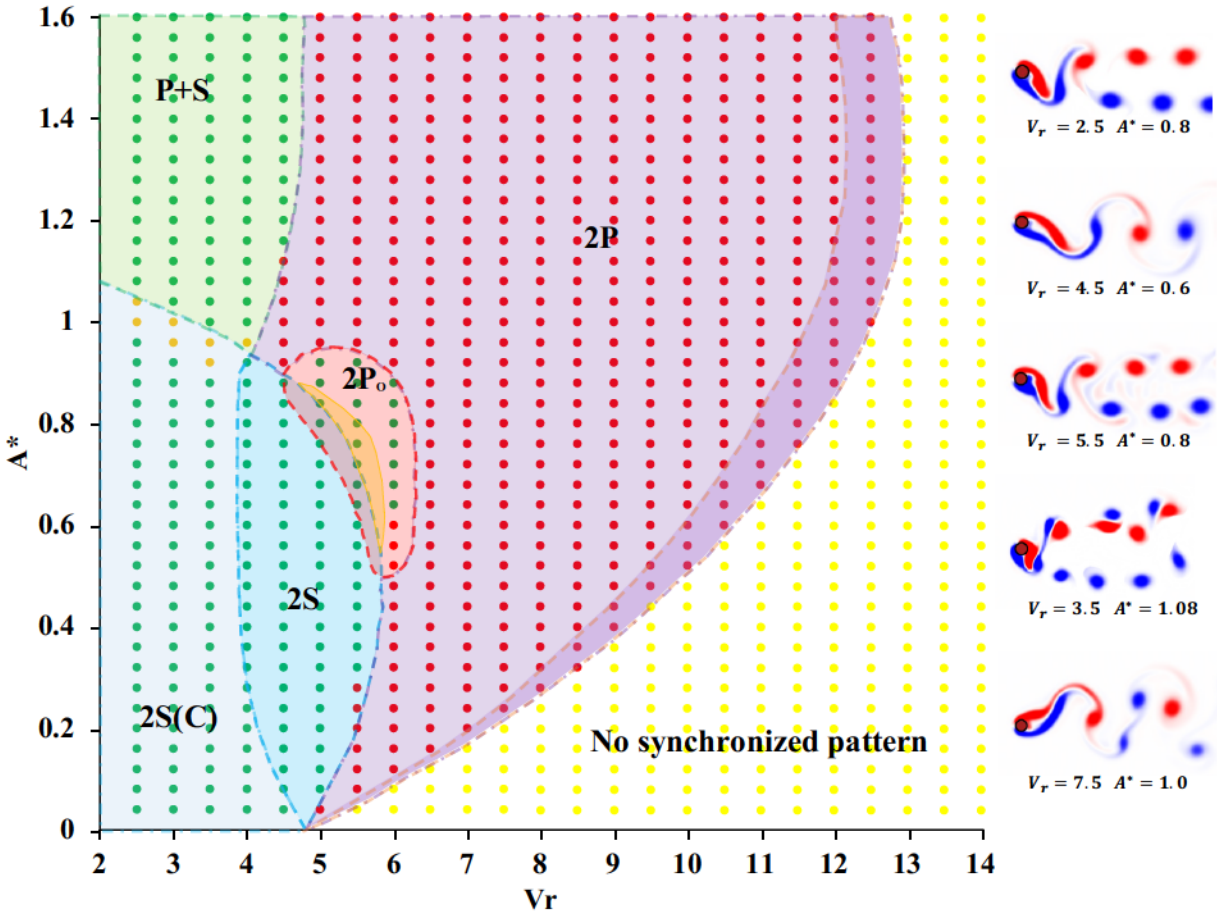

Fig. 1. Comparison of 2D simulations results with experimental data in the map of vortex-shedding regimes

In summary, the comparison between the 2D simulations and experimental data confirms the relatively accurate agreement between the numerical results and experimental values in regions where valid wake modes are present. However, discrepancies are observed in the 2P region, where the numerical simulation values deviate significantly from the experimental values. For instance, the right bottom wake mode in Fig. 1 depicts an incorrect simulated response in the 2P region. Fig. 3 presents a comparison between 2D simulation results and experimental data at $Vr = 4.4, A^* = 1.34$, concentrating on force-time traces and spectra for the P+S mode. Fig. 4 provides a similar comparison but for the 2S mode at $Vr = 3,\ A^* = 0.2$ including time traces, force spectra, and vorticity field. Both figures serve as prime examples demonstrating that 2D simulations effectively capture the experimental results in terms of force and wake modes. In summary, the comparison showcased in Fig. 3 and Fig. 4 highlights the ability of 2D simulations to accurately reproduce the experimental outcomes, particularly in terms of force characteristics and the formation of wake modes. These findings further validate the reliability and

efficacy of 2D simulations in capturing the complex dynamics associated with VIV in low V_r (2S and P+S regions).

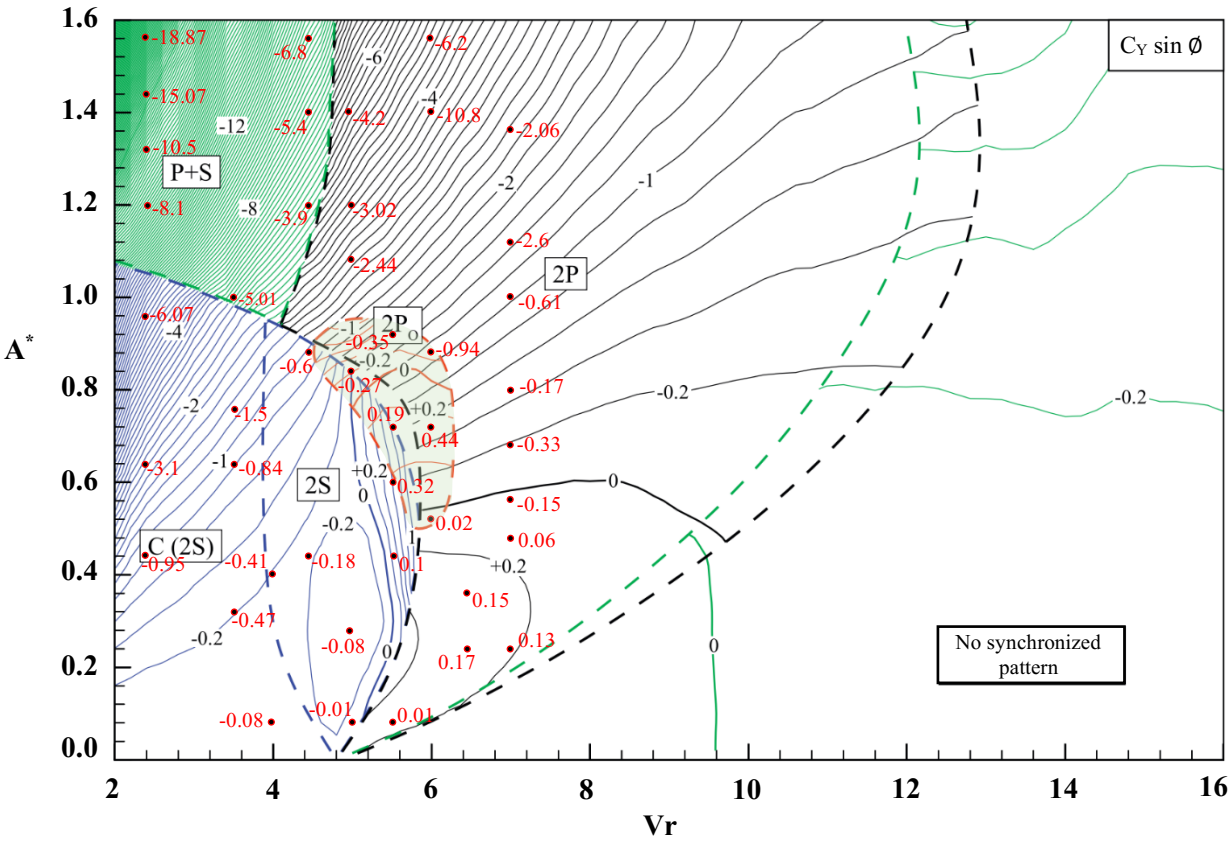

Fig. 2. Comparison of 2D simulations results with experimental data in the force in phase with velocity (Figure adapted from Morse and Williamson (2009))

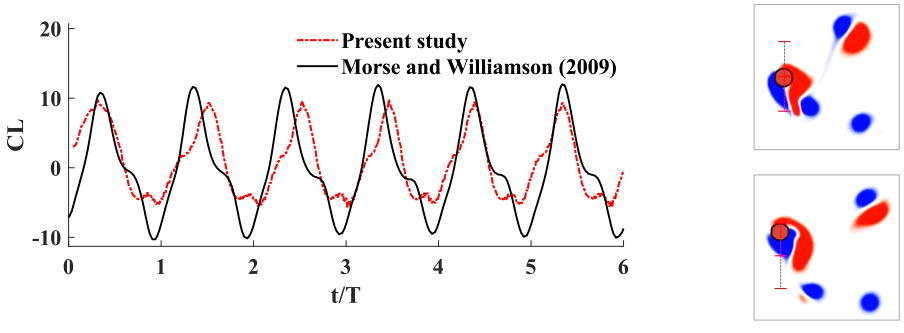

(a)

Fig. 3 (a). Comparison of 2D simulation results with experimental data in force time traces and spectra for P+S mode ($Vr = 4.4, A^* = 1.34$)

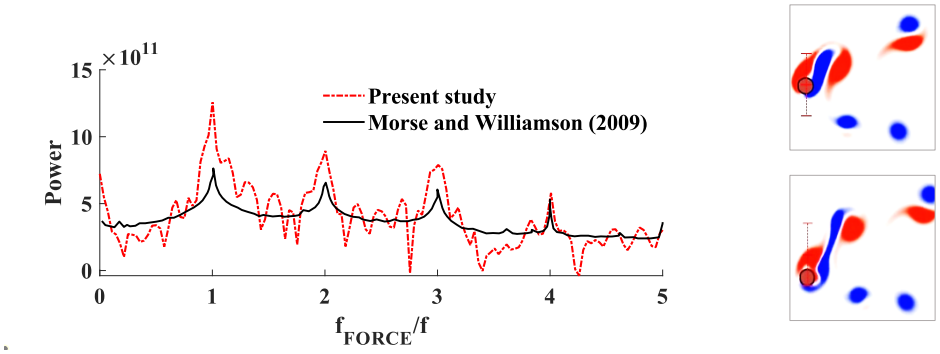

(b) (c)

Fig. 3 (b,c). Comparison of 2D simulation results with experimental data in force time traces and spectra for P+S mode ($Vr = 4.4, A^* = 1.34$)

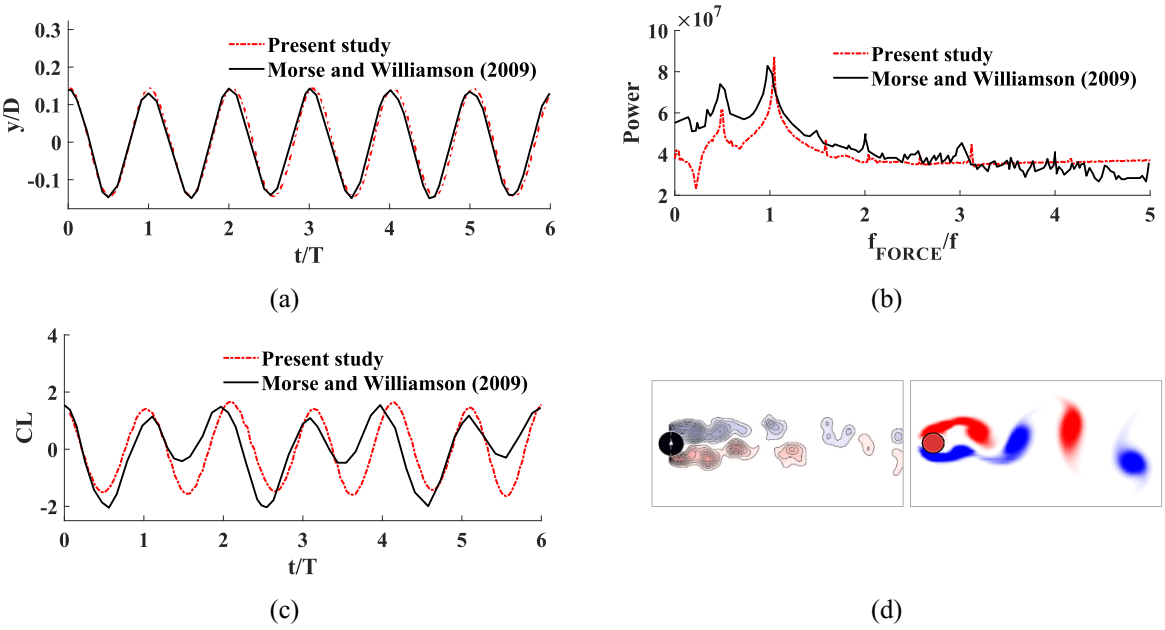

(a) (b)

(c) (d)

Fig. 4. Comparison of 2D simulation results with experimental data typical time traces, force spectra, and vorticity field for 2S mode of vortex formation ($Vr = 3, A^* = 0.2$)

4. Conclusions

This research study utilized the boundary data immersion method to perform real-time numerical simulations, aiming to investigate two-dimensional (2D) VIV. Specifically, our focus was on validating these simulations for the 1-DOF forced motion of a cylinder in a free stream. The results obtained from the simulations demonstrated a high degree of fidelity, as evidenced by the remarkable agreement with experimental data regarding wake patterns and forces. Notably, this agreement was particularly pronounced at low reduced velocities and low non-dimensional amplitudes. Nevertheless, as we increased the reduced velocity and amplitude, the influence of three-dimensional (3D) effects

became increasingly pronounced. Consequently, the limitations of the 2D simulations in accurately capturing these effects became evident. Thus, it is imperative to gain a comprehensive understanding of the conditions that trigger the onset of 3D effects to develop precise prediction models. This knowledge is essential for enhancing the accuracy of future predictions. Overall, our research successfully validated the efficacy of 2D simulations for modeling vortex-induced vibrations, particularly under conditions characterized by low velocities and amplitudes. However, the limitations associated with capturing 3D effects using 2D simulations underscore the need for further investigation into the underlying conditions that give rise to these effects. By acquiring a deeper understanding of these conditions, we can enhance the accuracy of prediction models for VIV, thereby facilitating improved design and analysis in relevant engineering applications.

References

Aktosun, E., Gedikli, E. D., & Dahl, J. M. (2023). Observed Wake Branches from the 2-Dof Forced Motion of a Circular Cylinder in a Free Stream [Preprint]. SSRN.

Aspden, A., Nikiforakis, N., Dalziel, S., & Bell, J. (2008). Analysis of implicit LES methods. Communications in Applied Mathematics and Computational Science, 3(1), 103–126.

Bearman, P. W. (1984). Vortex Shedding from Oscillating Bluff Bodies. Annual Review of Fluid Mechanics, 16(1), 195–222.

Bearman, P. W. (2011). Circular cylinder wakes and vortex-induced vibrations. Journal of Fluids and Structures, 27(5–6), 648–658.

Carberry, J., Sheridan, J., & Rockwell, D. (2005). Controlled oscillations of a cylinder: Forces and wake modes. Journal of Fluid Mechanics, 538(1), 31.

Font Garcia, B., Weymouth, G. D., Nguyen, V.-T., & Tutty, O. R. (2019). Span effect on the turbulence nature of flow past a circular cylinder. Journal of Fluid Mechanics, 878, 306–323.

Gabbai, R. D., & Benaroya, H. (2005). An overview of modeling and experiments of vortex-induced vibration of circular cylinders. Journal of Sound and Vibration, 282(3–5), 575–616.

Gedikli, E. D., & Dahl, J. M. (2014). Mode Shape Variation for a Low-Mode Number Flexible Cylinder Subject to Vortex-Induced Vibrations. Volume 2: CFD and VIV, V002T08A071.

Gopalkrishnan, R. (1993). Vortex-induced forces on oscillating bluff cylinders.

Griffin, O. M., & Ramberg, S. E. (1982). Some Recent Studies of Vortex Shedding With Application to Marine Tubulars and Risers. Journal of Energy Resources Technology, 104(1), 2–13.

Jiang, H., Cheng, L., & An, H. (2018). Three-dimensional wake transition of a square cylinder. Journal of Fluid Mechanics, 842, 102–127.

Maertens, A. P., & Weymouth, G. D. (2015). Accurate Cartesian-grid simulations of near-body flows at intermediate Reynolds numbers. Computer Methods in Applied Mechanics and Engineering, 283, 106–129.

Morse, T. L., & Williamson, C. H. K. (2009). Fluid forcing, wake modes, and transitions for a cylinder undergoing controlled oscillations. Journal of Fluids and Structures, 25(4), 697–712.

Pan, Z. Y., Cui, W. C., & Miao, Q. M. (2007). Numerical simulation of vortex-induced vibration of a circular cylinder at low mass-damping using RANS code. Journal of Fluids and Structures, 23(1), 23–37.

Parkinson, G. (1989). Phenomena and modelling of flow-induced vibrations of bluff bodies. Progress in Aerospace Sciences, 26(2), 169–224.

Sarpkaya, T. (1979). Vortex-Induced Oscillations: A Selective Review. Journal of Applied Mechanics, 46(2), 241–258.

Sarpkaya, T. (2004). A critical review of the intrinsic nature of vortex-induced vibrations. Journal of Fluids and Structures, 19(4), 389–447.

Vikestad, K., Vandiver, J. K., & Larsen, C. M. (2000). Added mass and oscillation frequency for a circular cylinder subjected to vortex-induced vibrations and external disturbance. Journal of Fluids and Structures, 14(7), 1071–1088.

Weymouth, G. D. (2014). Chaotic rotation of a towed elliptical cylinder. Journal of Fluid Mechanics, 743, 385–398.

Weymouth, G. D. (2015). Lily Pad: Towards Real-time Interactive Computational Fluid Dynamics.

Weymouth, G. D., & Yue, D. K. P. (2011). Boundary data immersion method for Cartesian-grid simulations of fluid-body interaction problems. Journal of Computational Physics, 230(16), 6233–6247.

Williamson, C. H. K. (1996). Three-dimensional wake transition. Journal of Fluid Mechanics, 328, 345–407.

Williamson, C. H. K., & Govardhan, R. (2004). V ORTEX -I NDUCED V IBRATIONS. Annual Review of Fluid Mechanics, 36(1), 413–455.

Williamson, C. H. K., & Govardhan, R. (2008). A brief review of recent results in vortex-induced vibrations. Journal of Wind Engineering and Industrial Aerodynamics, 96(6–7), 713–735.

Yang, W., & Stremler, M. A. (2016). Two-dimensional wakes of an oscillating cylinder at low Reynolds number.